

## The application of an Improved d.c. Polarization Technique to the Electronic Conductivity Measurements of $\alpha$ -AgI and AgBr

Junichiro MIZUSAKI, Kazuo FUEKI, and Takashi MUKAIBO

*Department of Industrial Chemistry, Faculty of Engineering, The University of Tokyo, Hongo, Bunkyo-ku, Tokyo 113*

(Received June 27, 1977)

An improvement was made in the d.c. polarization technique which is used for the measurement of the electronic conductivity of solid electrolytes. In the electrochemical cell, Ag/AgX (X=Br or I)/carbon, the carbon electrode was sealed with AgX in the bottom of a Pyrex tube so that the electrode reaction at the AgX/carbon interface could be suppressed in the steady state. Using the improved d.c. polarization cell, measurement was made of the electronic conductivity of AgI in the temperature range from 330 to 500 °C, and that of AgBr, at temperatures from 375 to 400 °C, as a function of the halogen partial pressure,  $P_{X_2}$ . It was found that the electronic conduction of  $\alpha$ -AgI is  $p$ -type and that the electronic conductivity is proportional to  $P_{I_2}^{1/2}$ . The electronic conductivity of AgBr was found to be proportional to  $P_{Br_2}^{-1/2}$  in a low-pressure range of bromine, and proportional to  $P_{Br_2}^{1/2}$  in a high-pressure range.

Hebb-Wagner's d.c. polarization technique<sup>1,2)</sup> is generally used for the determination of the electronic conductivity of solid electrolytes. For the determination of electronic conductivity by this technique, a complete blocking of the ionic current is necessary. Thus far, the following two types of cell arrangement have been employed for the measurement of AgI and AgBr:

- (I)  $\ominus$  Ag/AgX/carbon, inert atmosphere  $\oplus$
- (II)  $\ominus$  carbon, inert atmosphere/AgX/carbon, halogen gas atmosphere  $\oplus$

where AgX denotes AgI or AgBr. However, in these cells the ionic current can not be blocked completely, because one of the carbon electrodes is open to the inert atmosphere, and the chemical equilibrium can not be established at the electrode/AgX interface.

Using a cell of Type (I), Ilschner<sup>3)</sup> measured the electronic conductivity of AgI and AgBr and found that AgI shows the  $p$ -type electronic conduction in the temperature range from 267 to 332 °C, but the slope of the logarithmic plots of the current against the applied potential difference was 1.2 times larger than that expected by Wagner's theory.<sup>2)</sup> Above 332 °C, the electronic conductivity could not be determined because of the increased decomposition current. In the case of AgBr, the  $n$ -type conduction was observed under the small applied potential difference in the temperature range from 333 to 372 °C, but the decomposition current increased with the increase in the applied potential difference.

Raleigh investigated the electronic conduction of AgBr at temperatures between 250 and 400 °C using a cell of Type (II); he observed both  $n$ - and  $p$ -type conductions, in accordance with the applied potential difference, but the decomposition current became large with a decrease in the applied potential difference.<sup>4)</sup>

As has been mentioned above, as to  $\alpha$ -AgI (stable above 146 °C) and AgBr, no work<sup>3-6)</sup> has succeeded in showing whether or not the relation between the current and the applied potential difference coincides with the prediction by Wagner's theory.

The purpose of the present study is to devise a d.c. polarization cell in which the decomposition current is completely blocked and to determine the electronic conductivity of  $\alpha$ -AgI and AgBr as a function of the halogen partial pressure.

### Improved d.c. Polarization Cell

A conventional d.c. polarization cell of Type (I) is shown in Fig. 1. In the cell, inert gas flows over the electrodes and carries halogen gas from the AgX/carbon interface. Therefore, a polarization cell of this type can not block the decomposition current completely.

In order to obtain a complete ion-blocking condition, the authors devised the d.c. polarization cell shown in Fig. 2. In this cell, AgX seals the carbon electrode completely in a small space at the bottom of a Pyrex tube. When an electrical potential difference is applied between the carbon (positive) and the silver (negative) electrodes, the partial pressure of halogen gas,  $P_{X_2}^*$ , in the space changes as a result of charging and discharging, finally reaching the value

$$P_{X_2}^* = P_{X_2}^\circ \exp\left(\frac{2FE}{RT}\right), \quad (1)$$

where  $P_{X_2}^\circ$  denotes the halogen partial pressure in equilibrium with the AgX co-existing with metallic silver and where  $E$  denotes the applied potential difference. Under this condition, the ionic current ceases to flow and Hebb-Wagner's d.c. polarization technique can be applied. We call a cell of this type an improved

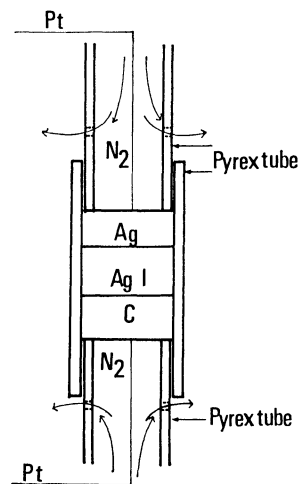


Fig. 1. Conventional type cell.

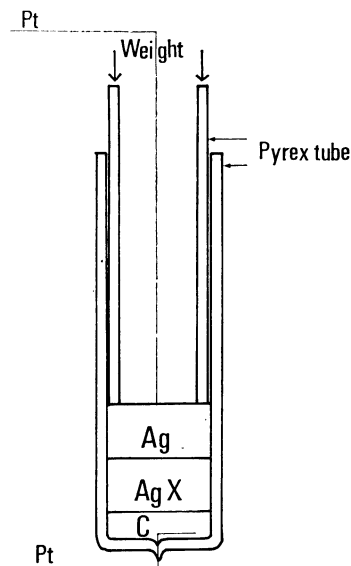


Fig. 2. Improved cell.

d.c. polarization cell.

Equation 1 can be rewritten as follows by using the silver chemical potential,  $\mu_{Ag}$ :

$$EF = \mu_{Ag}^{\circ} - \mu_{Ag}^{*}, \quad (2)$$

where  $\mu_{Ag}^{\circ}$  denotes  $\mu_{Ag}$  in AgX in equilibrium with metallic silver and where  $\mu_{Ag}^{*}$  is that of AgX at the AgX/carbon interface. Using the silver activity,  $a_{Ag}$ , we obtain

$$EF = -RT \ln a_{Ag}^{*}, \quad (3)$$

where  $a_{Ag}^{*}$  denotes the  $a_{Ag}$  in AgX at the AgX/carbon interface and where the  $a_{Ag}$  in AgX co-existing with metallic silver is taken as unity.

### Experimental

**Cells and Samples.** In order to compare the improved cell with the conventional-type cell, measurements were carried out using both types of cells (Figs. 1 and 2). The cells were constructed in a Pyrex tube, 10 mm in inner diameter. The silver electrode, carbon electrode, and AgX pellet used were the same as those used in a previous work.<sup>7)</sup> The AgX pellet was sandwiched by the silver and carbon electrodes and pressed by means of a spring to ensure contact. In a conventional-type cell, purified nitrogen gas was let flow over the surface of the electrodes. In an improved cell, a Pt lead wire was sealed at the lower end of the Pyrex tube. Then the cell was heated at about 400 °C so that the AgX pellet could deform plastically by a slight pressure and come in close contact with the wall of the Pyrex tube. Thus, the carbon electrode was completely sealed in a small space.

**Coulometric Study.** Prior to the construction of the cells, the weights of the silver electrode and the AgI pellet were measured. After the cell construction, a constant potential difference of 400 or 450 mV was applied at 500 °C for several days. The current decay was recorded by means of an electric recorder. The electricity passed through the cell was calculated by integrating the current-time curve. Then, the cell was disassembled and the weights of the silver electrode and AgI pellet were measured again.

**Measurement of the Current and Potential in the Steady State.** Measurements were performed at temperatures from 330 to

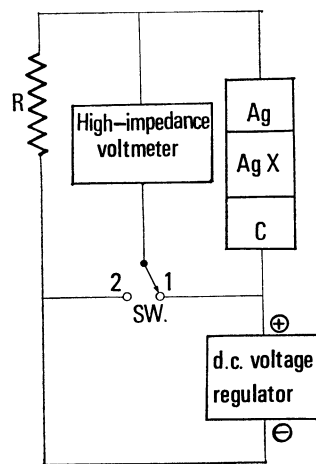


Fig. 3. Circuit diagram for the measurement.

$$R = 100 \, \Omega - 10 \, k\Omega$$

500 °C for AgI, and at 375 and 400 °C for AgBr, by the use of the improved cell. For comparison, a conventional-type cell was also used for AgI at 500 °C. When the steady state current exceeds about 5  $\mu$ A, the measurement could be carried out by applying a constant potential difference between the electrodes by means of a d.c. voltage regulator. However, current fluctuation was caused even in the steady state by the unavoidable slight fluctuations in the temperature or the applied potential difference. This current fluctuation became a serious obstacle to the measurement when the steady-state current was lower than about 5  $\mu$ A. The use of the circuit shown in Fig. 3 was found to be very effective in avoiding such difficulty, and so it was mainly employed in the present work. In this circuit, the standard resistance,  $R$ , was connected in series with the cell, and a constant potential difference was applied between the two ends of the series. The resistance showed a kind of buffer action on the fluctuation. When  $E$  deviated positively from the relation in Eq. 1, the drop in the current or the ohmic value due to the resistance increased. Consequently, the potential difference loaded to the cell  $E$  decreased. Thus, the fluctuation was dampened. When the value of  $R$  was chosen so that the ohmic drop at this resistance was 1 to 10% of the applied potential difference in the steady state, the fluctuation of the current and  $E$  was effectively suppressed.

The current passed through the cell was determined from the ohmic drop at the resistance measured by means of a high-impedance voltmeter, which was also used for the measurement of the applied potential difference between the electrodes. The steady state was confirmed from the current and potential difference, which had been kept constant for at least 2 or 3 h.

The electric furnace and the temperature-controlling system were already described in a previous paper.<sup>7)</sup>

### Results and Discussion

**Comparison of the Improved Cell with the Conventional-type One.** The results of coulometry using both types of cells are shown in Table 1. When AgI is electrolysed, silver deposits on the silver electrode and iodine gas is released in the nitrogen atmosphere or diffuses into the carbon electrode. Therefore, the change in the sum of the weights of the silver electrode and the AgI pellet is equal to the quantity of iodine gas released by the electrolysis. The difference between the quantity

TABLE 1. ESTIMATION OF THE RATIO OF THE DECOMPOSITION CURRENT TO THE ELECTRONIC CURRENT

	Conventional-type cell		Improved cell	
	Run 1	Run 2	Run 11	Run 12
$E/\text{mV}$	450	400	450	400
Quantity of electricity passed through the cell; $[A]/\text{Faraday}$	$1.90 \times 10^{-3}$	$1.20 \times 10^{-3}$	$11 \times 10^{-4}$	$55 \times 10^{-5}$
Initial weight/g of sample				
Ag	2.41	2.65	2.72	7.37
AgI	1.51	1.43	1.37	1.66
Ag+AgI	3.93	4.08	4.09	9.02
Final weight/g of sample				
Ag+AgI	3.74	3.94	4.07	9.01
Weight loss/g	0.19	0.14	0.02	0.01
Released iodine; $[B]/\text{eqv.}$	$1.5 \times 10^{-3}$	$1.1 \times 10^{-3}$	$2 \times 10^{-4}$	$8 \times 10^{-5}$
The ratio; $[B]/([A]-[B])$	3.8	$1.1 \times 10$	0.2	0.2

of the electricity passed through the cell in Faraday,  $[A]$ , and the quantity of released iodine in the equivalent,  $[B]$ , is equal to the quantity of electricity carried by the electrons. Thus,  $[B]/([A]-[B])$  gives the ratio of the decomposition current to the electronic current. As is clearly shown in Table 1, the decomposition current is predominant in the conventional-type cell, while the electronic current is predominant in the improved cell.

It should be noted that even when an improved cell is used, the electrolysis of AgI occurs until the carbon electrode is saturated with iodine gas with a partial pressure of  $P_{I_2}^*$ . The weight loss and the quantity of electricity, due to the electrolysis, are included in the values in Table 1. In the steady state, ion blocking would be effected more completely than that indicated in Table 1.

According to Wagner,<sup>2)</sup> when AgX shows a  $p$ -type electronic conduction and when the electronic conductivity due to electron holes is expressed by Eq. 4, the relation between the current density,  $I$  and  $E$  under the complete ion-blocking condition can be represented by Eq. 5:

$$\sigma_h = \sigma_h^\circ \exp\left(\frac{\mu_{Ag}^\circ - \mu_{Ag}}{RT}\right), \quad (4)$$

$$\frac{IFL}{RT} = \sigma_h^\circ \left\{ \exp\left(\frac{EF}{RT}\right) - 1 \right\}, \quad (5)$$

where  $\sigma_h$  denotes the electronic conductivity in AgX, the silver chemical potential of which is kept at  $\mu_{Ag}$ , where  $\sigma_h^\circ$  denotes the  $\sigma_h$  of AgX in equilibrium with the metallic silver, and where  $L$  denotes the thickness of the AgX pellet. In the previous paper,<sup>7)</sup> the authors showed, by the measurement of the chemical potential profile, that Eq. 5 holds for AgI at 500°C.

When  $EF \gg RT$ , Eq. 5 can be rewritten as

$$\frac{IFL}{RT} = \sigma_h^\circ \exp\left(\frac{EF}{RT}\right), \quad (6)$$

that is

$$\log \frac{IFL}{RT} = \log \sigma_h^\circ + \frac{EF}{2.303RT}. \quad (7)$$

Therefore, if the decomposition current is completely blocked, the slope of the log  $I$ - $E$  plot should be  $F(2.303$

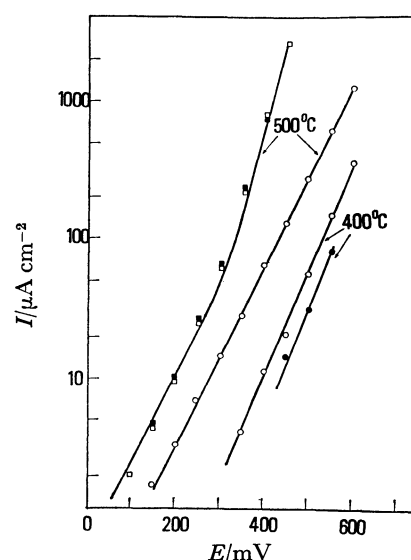


Fig. 4. Plots of  $I$  vs.  $E$  for AgI.

□: Conventional type cell,  $L=2.7$  mm, ■: conventional type cell,  $L=6.0$  mm, ○: improved cell,  $L=3.3$  mm, ●: improved cell,  $L=6.5$  mm.

$RT)^{-1}$  and  $I$  should depend on  $L$ . However, if the decomposition current is predominant,  $I$  should be independent of  $L$ .

The plots of the logarithm of  $I$  against  $E$  in the steady state, obtained by the use of both types of cells, are shown in Fig. 4. When the conventional-type cell is used, the slope of the plots is equal to  $F(2.303RT)^{-1}$  in the  $E < 300$  mV region, while in the  $E > 300$  mV region the slope is  $2F(2.303RT)^{-1}$ . The current density is independent of  $L$ . When the improved cell is used, the slope of the plots is  $F(2.303RT)^{-1}$  and is independent of  $E$ . The current density depends on  $L$ .

Those results indicate that the improved cell blocks the ionic current completely in the steady state and that the improved cell makes it possible to apply the d.c. polarization technique even when the conventional-type cell can not be used because of the predominant decomposition current.

The results obtained by means of the improved cell will be given below.

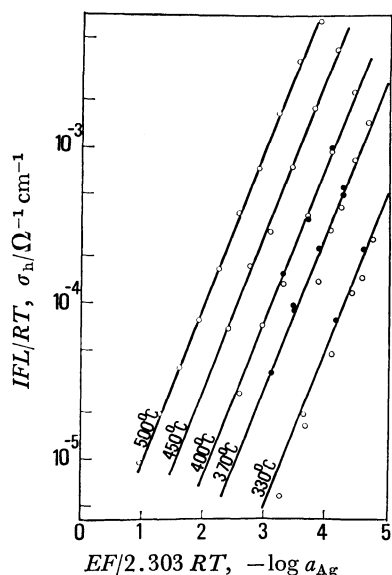


Fig. 5. Plots of  $\sigma_h$  vs.  $\log a_{Ag}$  for AgI.  
 ○:  $L=3.8$  mm, ●:  $L=6.5$  mm.

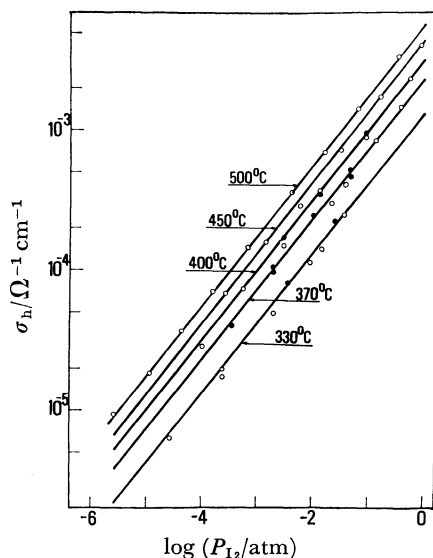


Fig. 6. Plots of  $\sigma_h$  vs.  $\log P_{I_2}$  for AgI.  
 ○:  $L=3.8$  mm, ●:  $L=6.5$  mm.

**Electronic Conductivity of  $\alpha$ -AgI.** The results for AgI are given in Fig. 5 as a semi-logarithmic plot of  $IFL(RT)^{-1}$  against  $EF(2.303RT)^{-1}$ . Using Eqs. 2, 4, and 6, we obtain

$$\sigma_h^* = \frac{IFL}{RT}, \quad (8)$$

where  $\sigma_h^*$  is the electronic conductivity of AgI at the AgI/carbon interface. By the help of Eq. 3,  $EF(2.303RT)^{-1}$  can be substituted for  $\log a_{Ag}^*$ . Therefore, Fig. 5 also indicates the plots of  $\sigma_h$  against the  $a_{Ag}$  of AgI. The combination of Eqs. 1 and 3 yields

$$\log a_{Ag}^* = -\frac{1}{2} \log \frac{P_{I_2}^*}{P_{I_2}^\circ}. \quad (9)$$

Thus,  $\log a_{Ag}^*$  can be expressed in terms of  $P_{I_2}^*$ . The plots of  $\sigma_h$  against  $P_{I_2}$  are shown in Fig. 6. The thermodynamic data summarized by Worrell and Hladik<sup>8)</sup>

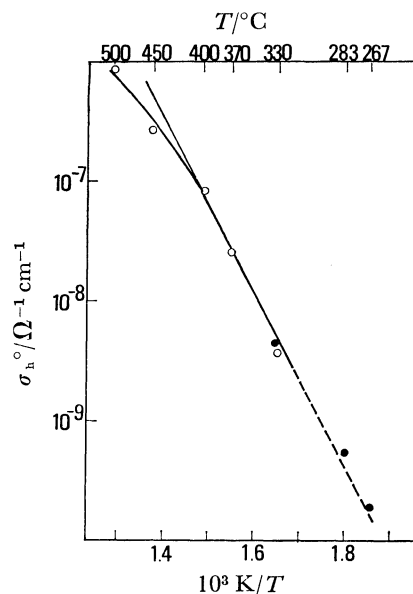


Fig. 7. Arrhenius plots of  $\sigma_h^0$  for AgI.  
 ○: This work, ●: by Ilschner.

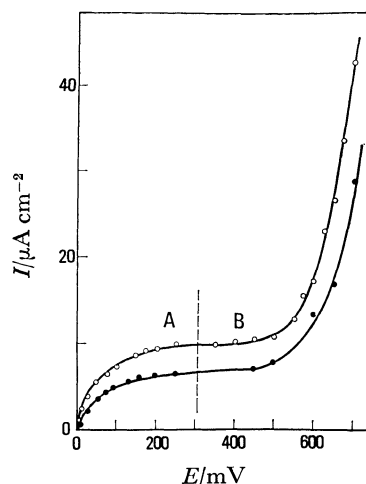


Fig. 8. Plots of  $I$  vs.  $E$  for AgBr at 400 °C.  
 ○:  $L=2.2$  mm, ●:  $L=3.3$  mm.

are used for the calculation of  $P_{I_2}^\circ$  in Eq. 9. We can see from Fig. 6 that the  $\sigma_h$  of AgI is proportional to  $P_{I_2}^{1/2}$ .

The plots of  $\sigma_h^0$  against  $T^{-1}$  are shown in Fig. 7. In the figure, the  $\sigma_h^0$  values obtained by Ilschner<sup>3)</sup> by the use of the conventional-type cell in a lower temperature range are also shown for the sake of comparison. The two sets of data agree well with each other. The data for the  $\sigma_h^0$  of AgI in the temperature range from 267 to 400 °C are expressed as

$$\sigma_h^0 = 2.76 \times 10^3 \exp(-1.64 \times 10^4 T^{-1}) \text{ (ohm}^{-1} \text{ cm}^{-1}\text{)}. \quad (10)$$

Above 400 °C, the Arrhenius plot for  $\sigma_h^0$  is curved. The reason for this is not clear, since the drift mobility or the concentration of electron holes have not been measured in this temperature range.

**Electronic Conductivity of AgBr.** The plots of  $I$  against  $E$  at 400 °C are shown in Fig. 8. In the present results,  $I$  is proportional to  $L^{-1}$ , so a complete ion

blocking is indicated. The curve can be divided into two parts, A and B. In Part A ( $E < 300$  mV)  $I$  asymptotically reaches a plateau,  $I_{pl}$ , while in Part B ( $E > 300$  mV)  $I$  increases exponentially from the plateau. It is known that AgBr shows an  $n$ -type electronic conduction when  $E < 300$  mV<sup>7)</sup> and shows a  $p$ -type electronic conduction when the equilibrium bromine partial pressure is high. Therefore, Part A may correspond to the  $n$ -type region, and Part B to the region in which the  $p$ -type electronic conduction is predominant.

According to Wagner,<sup>2)</sup> when the electronic conductivity of AgBr due to the conduction electrons is expressed by Eq. 11, the  $I$ - $E$  relation under the complete ion-blocking condition can be represented by Eq. 12;

$$\sigma_e = \sigma_e^\circ \exp\left(\frac{\mu_{Ag} - \mu_{Ag}^\circ}{RT}\right), \quad (11)$$

$$\frac{IFL}{RT} = \sigma_e^\circ \left\{ 1 - \exp\left(-\frac{EF}{RT}\right) \right\}. \quad (12)$$

Here,  $\sigma_e$  denotes the electronic conductivity at  $\mu_{Ag}$ , while  $\sigma_e^\circ$  denotes the  $\sigma_e$  of AgBr in equilibrium with metallic silver. The authors showed in the previous paper<sup>7)</sup> that Eq. 12 holds for AgBr in the temperature range from 350 to 400 °C when  $E < 300$  mV.

Equation 12 indicates that, when  $EF \gg RT$ ,  $I$  is equal to a constant value,  $I_{pl}$ , that is,

$$\frac{I_{pl}FL}{RT} = \sigma_e^\circ. \quad (13)$$

Using Eqs. 12 and 13, we obtain

$$\frac{(I_{pl} - I)}{RT} = \sigma_e^\circ \exp\left(-\frac{EF}{RT}\right), \quad (14)$$

or

$$\log \frac{(I_{pl} - I)FL}{RT} = \log \sigma_e^\circ - \frac{EF}{2.303RT}. \quad (15)$$

The semi-logarithmic plots of  $(I_{pl} - I)FL(RT)^{-1}$  against  $EF(2.303RT)^{-1}$  for Part A are shown in Fig. 9. The data fall on a straight line with a slope of  $-1$ . Clearly, the present results obey Eq. 15. This confirms that Eq. 11 holds for AgBr when  $E < 300$  mV.

On the assumption that Eq. 4 holds for AgBr under the conditions of complete ion blocking and when  $E > 300$  mV, we obtain<sup>2)</sup>

$$\frac{IFL}{RT} = \sigma_e^\circ + \sigma_h^\circ \exp\left(\frac{EF}{RT}\right). \quad (16)$$

Using Eq. 13, we obtain

$$\frac{(I - I_{pl})FL}{RT} = \sigma_h^\circ \exp\left(\frac{EF}{RT}\right), \quad (17)$$

or

$$\log \frac{(I - I_{pl})FL}{RT} = \log \sigma_h^\circ + \frac{EF}{2.303RT}. \quad (18)$$

The semi-logarithmic plots of  $(I - I_{pl})FL(RT)^{-1}$  against  $EF(2.303RT)^{-1}$  for Part B are also shown in Fig. 9. The slope of the plots is unity. Therefore, Eq. 18 holds when  $E > 300$  mV. This result indicates that the electronic conduction in AgBr under a high bromine partial pressure can be well interpreted as the predominant electron-hole conduction expressed by Eq. 4.

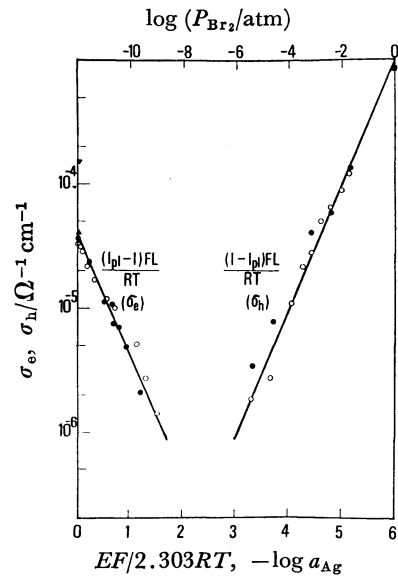


Fig. 9. Plots of  $\sigma_e$  and  $\sigma_h$  vs.  $\log a_{Ag}$  and  $\log P_{Br_2}$  at 400 °C for AgBr.  
○:  $L=2.2$  mm, ●:  $L=3.3$  mm, ▼: by Weiss, ▲; by Ilschner, ■: by Raleigh.

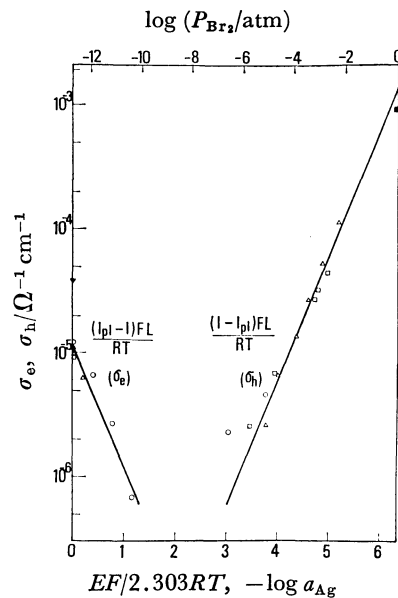


Fig. 10. Plots of  $\sigma_e$  and  $\sigma_h$  vs.  $\log a_{Ag}$  and  $\log P_{Br_2}$  at 375 °C for AgBr.  
△:  $L=2.5$  mm, □:  $L=1.3$  mm, ○:  $L=2.2$  mm, ▼: by Weiss, ▲: by Ilschner, ■: by Raleigh.

By inserting Eq. 2 into Eqs. 14 and 17 respectively, we obtain

$$\frac{(I_{pl} - I)FL}{RT} = \sigma_e^* \quad (19)$$

and

$$\frac{(I - I_{pl})FL}{RT} = \sigma_h^*, \quad (20)$$

where  $\sigma_e^*$  and  $\sigma_h^*$  denote the  $\sigma_e$  and  $\sigma_h$  of AgBr at the AgBr/carbon interface respectively. Using Eqs. 1 and 3,  $EF(2.303RT)^{-1}$  is rewritten in terms of  $\log a_{Ag}^*$  and  $\log P_{Br_2}^*$ . Figure 9 shows the plots of  $\sigma_e$  and  $\sigma_h$  against  $\log a_{Ag}$  and  $\log P_{Br_2}$ . The corresponding values

of  $\log a_{\text{Ag}}$  and  $\log P_{\text{Br}_2}$  are also shown in Fig. 9. For the calculation of  $P_{\text{Br}_2}$ , the data in the literature were employed.<sup>8)</sup>

The results at 375 °C are shown in Fig. 10. Also, Figs. 9 and 10 show the  $\sigma_e^\circ$  values obtained by Ilschner<sup>3)</sup> and Weiss<sup>5)</sup> and the  $\sigma_h$  ( $P_{\text{Br}_2}=1$  atm) obtained by Raleigh<sup>4)</sup> by the use of conventional-type cells. The data by Ilschner and by Raleigh are in good agreement with the present results.

From the results presented above, it may be concluded that the improved cell can achieve complete ion blocking and that the electronic conductivity of silver halides can be determined strictly even under when the conventional-type cell can not be used.

### Summary

(1) In order to block the ionic current completely in the Hebb-Wagner d.c. polarization cell, an improved cell assembly was devised and used for the accurate determination of the electronic conductivity of  $\alpha$ -AgI

and AgBr.

(2) The electronic conductivity of  $\alpha$ -AgI (330 to 500 °C) was found to be proportional to  $P_{\text{I}_2}^{1/2}$ , and  $\sigma_h^\circ$  (267 to 400 °C) is expressed as:

$$\sigma_h^\circ = 2.76 \times 10^3 \exp(-1.64 \times 10^4 T^{-1}) \quad (\text{ohm}^{-1} \text{cm}^{-1})$$

The electronic conductivity of AgBr at 375 and 400 °C was found to be proportional to  $P_{\text{Br}_2}^{-1/2}$  in the low-pressure range of bromine, and proportional to  $P_{\text{Br}_2}^{1/2}$  in the high-pressure range.

### References

- 1) M. Hebb, *J. Chem. Phys.*, **20**, 185 (1952).
- 2) C. Wagner, *Proc. C. I. T. C. E.*, **7**, 361 (1955).
- 3) B. Ilschner, *J. Chem. Phys.*, **28**, 1109 (1958).
- 4) D. O. Raleigh, *J. Phys. Chem. Solids*, **26**, 329 (1965).
- 5) K. Weiss, *Z. Phys. Chem.*, **NF59**, 242 (1968).
- 6) K. Weiss, *Electrochim. Acta*, **16**, 201 (1971).
- 7) J. Mizusaki, K. Fueki, and T. Mukaibo, *Bull. Chem. Soc. Jpn.*, **48**, 428 (1975).
- 8) W. L. Worrell and J. Hladik, "Physics of Electrolyte," ed by J. Hladik, Academic Press, London-New York (1972), p. 747.